MODELING LAND-SURFACE ALBEDOS FROM VEGETATION CANOPY ARCHITECTURE

Clinton M. Rowe
Department of Geography
University of Nebraska
Lincoln, Nebraska 68588-0135

Abstract: Over the past decade, the climatic impact of changes in terrestrial albedo has been studied using numerous climate models, ranging from simple, one-dimensional energy balance climate models to the more sophisticated, three-dimensional general circulation models of the atmosphere. In most of these, however, the land-surface albedos have been prescribed both spatially and temporally from albedo observations. To overcome the limitations of using prescribed land-surface albedos, a model of radiation transfer in plant canopies was used to predict vegetation albedos. Because of the model's reliance on the physical properties of the land-surface cover, it is able to account explicitly for albedo variations caused by factors both internal to and external from the vegetation canopy. The model is described and the results of simulations for three representative canopy types are discussed. The dependence of albedo on irradiance distribution predicted by the model agrees well with established theory. [Key words: albedo, modeling, vegetation canopy, climatology.]

INTRODUCTION

Surface albedo determines the proportion of incident solar radiation absorbed by the Earth's surface and, thus, the amount of energy available for heating the ground and lower atmosphere as well as for evaporating water. Specification of land-surface albedos has been shown to have a significant impact on climate simulation (Charney et al., 1977; Preuss and Geleyn, 1980; Potter et al., 1981). In most general circulation models (GCMs), however, land-surface albedo is simply prescribed both spatially and temporally. Carson (1982) summarized three commonly used methods of specifying the albedo of snow- and ice-free continental surfaces in GCMs: (1) a single, fixed value for all land surfaces or, alternatively, separate values for vegetated land and desert; (2) albedo as a function of latitude only; and (3) a specified geographical distribution of albedos. Temporal variation of albedos, except in areas of seasonal snowcover, is often ignored, or at best prescribed on a monthly or seasonal basis. These methods, unfortunately, cannot account for variations in land-surface albedo due to such factors as the spectral composition and angular distribution of incident radiation, the ratio of direct to diffuse irradiance, plant phenology (especially leaf emergence, senescence, and drop), snow depth and age, and soil moisture.

Physical Geography, 1991, **12**, 2, pp. 93–114.

In their review of the albedo requirements of climate models, Henderson-Sellers and Wilson (1983, p. 1744) state that:

> if climate models are to be used to predict the effects of major climatological disturbances, such as the impact of increasing atmospheric CO_2, it is essential that (1) their sensitivity to surface albedo specification be rationalized and related to the real world and (2) a consistent global data set of surface albedo information of high accuracy be made available as soon as possible.

Although "it is tempting to rely on observational data for specifying surface albedos as prescribed constants in climate models" (Dickinson and Hanson, 1984), observations of land-surface albedos alone cannot be expected to provide the resolution necessary for climate simulation because of the nature of present observing techniques. Remote sensing, which yields observations over large areas, can provide estimates of surface albedo only under clear sky conditions. Moreover, except for geostationary satellites, remote sensing generally provides observations at only one time of day—precluding observation of diurnal variations of surface albedo. Geostationary satellites, while giving more frequent observations, at present have inadequate spatial resolution. Ground observations provide data under a wide range of conditions (e.g., both clear and cloudy skies) and can resolve diurnal variations, but give only point estimates of surface albedo. Numerical models, therefore, may provide better estimates of land-surface albedos for climate simulations than do current observations.

Dickinson (1983) proposed the use of a two-stream approximation (Coakley and Chylek, 1975; Meador and Weaver, 1980) to model the albedo of a vegetation canopy. Dickinson gives a solution for the albedo of a semi-infinite (i.e., optically dense) canopy composed of randomly distributed and uniformly oriented leaves. Sellers (1985) extended the two-stream approximation of Dickinson to sparse canopies by including the reflection of radiation from the soil surface and considering non-uniform leaf orientation distributions. Both Dickinson and Sellers assumed only a single scattering event for radiative flux within the canopy; that is, no multiple scattering between canopy elements was considered. This assumption may be appropriate for visible radiation (because of the large absorption coefficient of green vegetation at these wavelengths), but it could lead to large errors when modeling scattering in near-infrared wavelengths or from non-green vegetation (Dickinson, 1983).

The two-stream model is one-dimensional in nature; the canopy is considered to be horizontally homogeneous and of infinite extent, thereby eliminating edge effects. To apply the results of this model to more realistic, non-homogeneous vegetation canopies, a weighted average based on the relative proportions of ground covered by individual components is computed. For example, the albedo of a savanna with a 25 percent ground cover of deciduous trees would be obtained by weighting the albedo for deciduous forest by 0.25 and the albedo for grassland by 0.75 and then summing. This method totally misrepresents the three-dimensional nature of the savanna where individual trees or small groups of trees are scattered over a grassy plain. Weighted averaging implies that all the trees are grouped in a dense, homogeneous forest covering 25 percent of the savanna while

the remaining area is completely without tree cover. Since this method cannot account for light trapping due to the macro-structure of the vegetation (Federer, 1971; Dickinson, 1983), these weighted-average albedos generally overestimate the albedo of non-homogeneous vegetation canopies.

Kimes and Kirchner (1982) devised a model that explicitly considers horizontal inhomogeneity. In their model, the vegetation canopy is represented by a module that "characterize[s] the basic structural characteristics of the scene without repetition" (Kimes and Kirchner, 1982). This module is divided horizontally and vertically into cubes, which they called cells. For each cell, the required vegetation properties can be assigned. By including such information as the area density, angular distribution, spatial dispersion and optical properties of leaves, a ray tracing method similar to that of Cooper et al. (1982) can be extended to this three-dimensional model. Comparisons of simulated directional reflectance fields with measurements over a soybean crop show that this model is able to simulate the gross trends in the observations—at least for visible wavelengths (Kimes and Kirchner, 1982).

MODEL DESCRIPTION

The Kimes-Kirchner Model

The landscape for which albedo is to be simulated is first divided into modules defined by the user. Module size is dependent on the symmetry of the landscape; landscapes with highly repetitive structure (such as row crops and orchards) can be represented by smaller modules than can landscapes with less structure (such as forests or human-built environments). A module is composed of cells that contain the components (i.e., leaves, branches, trunks, open space) which comprise the landscape. Associated with each cell is information necessary to determine the interaction of radiation with the contents of that cell. Two scales of data are thus required to define the vegetation canopy for this model: (1) the large-scale structure of the canopy necessary to determine the size of the module and the cell contents and (2) the small-scale distribution of the vegetation components within each cell and their corresponding optical properties. In addition, the optical properties of the substrate underlying the canopy must be specified.

If only a single module were being considered, it would be necessary to know the radiation field surrounding the module on all sides and above the canopy. Kimes and Kirchner avoid this problem by assuming that the canopy is composed of adjacent modules that interact with the incident radiance in the same manner as the module being simulated; that is, the landscape is comprised of infinitely repeating modules. When radiation is predicted to exit one side of the module, an equivalent—in direction and magnitude—flux from an adjacent module enters the opposite side. Thus, radiation can enter and exit the canopy only through the top surface of the uppermost cell layer.

Radiative flux can arise from and be scattered into an infinite number of directions, making a full three-dimensional ray-tracing algorithm computationally prohibitive. To avoid this problem, the Kimes-Kirchner algorithm divides the

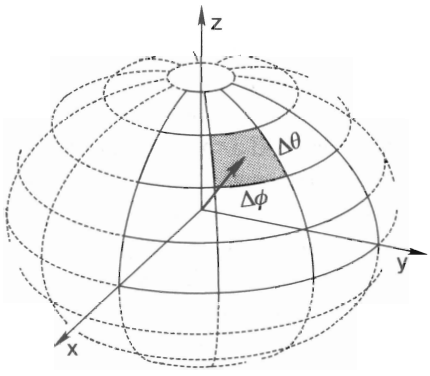

Fig. 1. Model coordinate system and radiation geometry. A spherical sector defined by azimuth ($\Delta\,\phi$) and inclination ($\Delta\,\theta$) intervals is shaded and the corresponding midvector is shown.

spherical coordinate system into a finite number of sectors (Fig. 1). These sectors are defined by constant azimuth ($\Delta\phi$) and inclination ($\Delta\theta$) intervals; the vectors between the origin and the midpoints of these sectors (midvectors) define the set of all possible directions for radiant flux in the model. Shortwave radiation—both direct and diffuse—is distributed among the sectors that define the sky hemisphere according to the position of the sun and the distribution of sky radiance. All the flux from a given sector is assumed to propagate along the midvector of that sector.

Flux that is unattenuated by the foliage in the cell continues along the same radiation flux vector into an adjacent cell. This process continues until the flux vector reaches the lowest layer of cells. At this point, any unattenuated flux leaving through the bottom of this layer will strike the underlying surface and either be absorbed or scattered upward (i.e., reflected). This entire process is repeated until every incident radiation flux vector striking each cell of the uppermost layer in the module has been traced from the canopy top to the underlying surface.

Interactions between shortwave radiation and the canopy are determined by following the path of the radiation through the cells which comprise the vegetation canopy module. Based on the information about the components of each cell, radiation either passes through the cell undisturbed or interacts with the vegetation elements. When radiation encounters a canopy element, a portion of the radiant flux is absorbed by the element and the remainder is scattered. Scattered flux is comprised of radiation reflected from and transmitted through the foliage elements.

Scattered flux arising from each cell in which an interaction occurred, as well as flux reflected from the substrate, is considered next. All scattered flux is assumed to originate from the center of the cell in which scattering took place or, for scattering from the substrate, from the center of the bottom surface of the lowest cell. The directions into which scattering can occur are again limited to those directions defined by the midvectors.

In the original version of their model, Kimes and Kirchner (1982) assumed isotropic scattering within the cells and from the substrate. This, in essence, treats the reflection and transmission coefficients of the foliage elements as equal and all foliage elements and the substrate as Lambertian reflectors. For stems and branches, as well as for thick leaves, the assumption of equal reflection and transmission is clearly in error, while the assumption of Lambertian reflection will not hold for some foliage elements (e.g., glaucous leaves). Kimes and Kirchner (1982) recognized that the isotropic assumption was weak and Kimes (1984) incorporated anisotropic scattering from leaves in a revised model.

Once the scattered fluxes for a canopy or substrate cell have been distributed among the midvectors, these vectors are traced through the module and their interactions with other cells are calculated. Fluxes exiting the module through the sides are assumed to enter an adjacent module while an identical, both in magnitude and direction, radiation flux vector enters the module under consideration from the opposite side. Thus, no flux can be lost through the sides or bottom of the module, only through the top. It is important to note that fluxes originating from within a canopy cell have no further interaction with that cell, while scattered fluxes beginning at the substrate are assumed to interact with the canopy cell immediately above them.

All scattered fluxes arising from every canopy and substrate cell are traced in this manner until they exit the canopy top or strike the underlying surface. Fluxes exiting the module through the top are accumulated. This process of tracing the scattered fluxes is continued until no radiation flux vector within the module has a magnitude greater than a predetermined threshold. Finally, the accumulated above-canopy, upward-directed flux is divided by the total incident flux to yield the module albedo.

Modifications to the Kimes-Kirchner Model

Although the present model is based largely on Kimes and Kirchner's (1982) radiative transfer model, it incorporates several significant modifications. First, the cells that comprise the canopy module do not have to be cubes. While Kimes and Kirchner required that these cells be cubes, the present implementation permits the cells to be formed by rectangular boxes of arbitrary—but constant for any one module—dimensions. This allows for a better representation of the different scales of variation often encountered in the vertical, compared to the horizontal, structure of the canopy. The assumption of cubic cells may be appropriate for the field crops considered by Kimes and Kirchner; for natural canopies, however, unequal cell dimensions are necessary. Second, systematic (regular or clumped) foliage dispersions are allowed in the present model; Kimes and Kirchner modeled random dispersions only. Even though little information on actual foliage dispersions exists, this extension provides flexibility should data become available. Third, Kimes and Kirchner considered leaves to be the only scattering and absorbing elements within the canopy. In the present model, both leaves and stems interact with radiation; other foliage elements (e.g., flowers and fruits) could be incorporated easily by simple extension of the model formulation. For natural

vegetation, stems may represent a large proportion of—and, sometimes, the only—plant surface area.

Finally, the two models differ in how they treat scattering from foliage elements. Kimes and Kirchner considered only isotropic scattering within the canopy, while Kimes (1984) incorporated anisotropic scattering from leaves using a scattering phase function. Hemispherically isotropic scattering is assumed in the present model, but the proportion of flux backscattered does not have to equal the proportion scattered into the forward hemisphere. While this parameterization is not as accurate as the scattering phase function for estimating directional reflectance used by Kimes (1984), it is more realistic than the completely isotropic scattering employed in the original Kimes-Kirchner model. The simple scattering phase function included in the present model defines, for each foliage type in a cell, a parameter that represents the proportion of scattered flux that is backscattered; that is, scattered into the hemisphere defined by the incident radiation flux vector and the plane normal to this vector (Fig. 2). For example, a backscatter parameter of 0.75 indicates that 75 percent of the radiation scattered by the foliage elements would be backscattered, while 25 percent would be forward scattered. This parameterization of scattering from foliage elements is a highly simplified representation of the actual scattering phase function, which is dependent on the reflection and transmission coefficients of the elements as well as the angle of incidence of the flux. All foliage elements are assumed to be isotropic scatterers, an assumption that will not hold for glaucous leaves, for example, although the effect on the total flux reflected by the canopy should be negligible. Reflection from the underlying surface is also assumed to be Lambertian, which could produce errors in the directional distribution of reflected flux, especially for a sparse vegetation cover. However, since total hemispherical reflectance—the albedo—is the desired model output, directional accuracy was sacrificed in favor of computational simplicity.

Model Implementation

While the modified ray tracing algorithm employed in this model is, in practice, no more than an elaborate bookkeeping procedure and will not be discussed further, the treatment of the interaction of radiation with the foliage elements in a cell requires some elaboration.

As radiation enters the top of the vegetation module along a source vector, it may interact with the vegetation elements contained in any cell through which it passes. The probability that radiation will pass through a cell without striking a foliage element is called the "probability of gap." The probability of gap, $P_0(\phi, \theta)$, expressed as a function of the direction (azimuth, ϕ; elevation, θ) of propagation, is dependent on the density, spatial dispersion and angular distribution of foliage elements (leaves, stems, etc.) in the cell and on the distance the radiation must travel through the cell—the path length.

Three types of foliage dispersion can be identified: random, regular or clumped (Warren Wilson, 1961; Nilson, 1971). A random dispersion means that the foliage elements are positioned independently of one another. When elements are

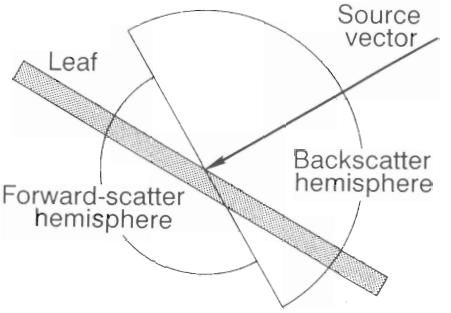

Fig. 2. Forward- and backscattering geometry. Isotropic scattering is assumed, but the proportions scattered forward and backward are not necessarily equal. Forward- and backscattered fluxes may include both reflected and transmitted radiation.

located preferentially in spaces left between other elements resulting in a lower probability of gap, the elements are regularly dispersed. Clumped elements increase the gap frequency. Each of these three dispersions requires the use of a separate probability distribution function to determine the gap frequency: Poisson, positive binomial and negative binomial for random, regular and clumped dispersions, respectively. These can be expressed as a function of foliage dispersion (F_d) by

$$P_0(\phi,\theta) = \exp[-LG(\phi,\theta)D] \tag{1}$$

$F_d = 0$, random dispersion

or

$$P_0(\phi,\theta) = \exp\{(L/F_d)\ln[1-G(\phi,\theta)D\,F_d]\} \tag{2}$$

$F_d > 0$, regular dispersion

$F_d < 0$, clumped dispersion

where L is the foliage area density ($m^2\ m^{-3}$), defined as the surface area (one side, projected into two dimensions for elements that are not flat) of foliage elements per unit canopy volume, D is the path length of the radiation flux vector through the cell (m) and $G(\phi, \theta)$ is the mean projection of unit foliage area in the direction of the radiation flux vector with azimuth ϕ and elevation θ (Nilson, 1971). This projection function, $G(\phi, \theta)$, is dependent on the angular distribution—inclination and azimuth—of the foliage elements and the direction of the radiation flux. It is expressed as

$$G(\phi,\theta) = \frac{1}{2\pi}\int_0^{2\pi}\int_0^{\frac{\pi}{2}} g(\phi_l,\theta_l)|\cos\xi|\sin\theta_l d\theta_l d\phi_l \tag{3}$$

where ϕ_l and θ_l are the foliage element azimuth and inclination angles, respectively, $g(\phi_l, \theta_l)$ is the distribution function of foliage orientation, and ξ is the angle between the normal to the foliage element and the radiation flux vector (Ross, 1975) determined by

$$\cos\xi = \cos\theta\cos\theta_l + \sin\theta\sin\theta_l\cos(\phi-\phi_l) \tag{4}$$

with the terms defined as for (3).

If the distribution function of foliage orientation, $g(\phi_l, \theta_l)$, is known, the projection function, $G(\phi, \theta)$, can be determined either analytically or numerically from (3). Except for a few crop canopies, however, $g(\phi_l, \theta_l)$ has not been evaluated and must be assumed instead. If there is no preferred azimuth for the foliage orientation (Ross, 1975), the projection function is dependent only on the foliage inclination angle distribution and the elevation of the radiation flux vector. A further simplification can be made by assuming an inclination angle distribution appropriate to the canopy. Three common assumptions are: (1) horizontal foliage, (2) vertical foliage, and (3) uniformly-distributed foliage. The projection functions for the these inclination angle distributions can be determined from (3) and are given by

$$G(\phi,\theta) = \begin{cases} |\sin\theta|, \textit{ horizontal} \\ 2\cos\theta/\pi, \textit{ vertical} \\ 1/2, \textit{ spherical} \end{cases} \tag{5}$$

When a specified foliage inclination distribution is used in conjunction with the assumption of azimuthal independence, the projection function is dependent only on the elevation angle of the radiation flux vector, θ.

Substituting $G(\phi,\theta)$ into the appropriate probability of gap function, (1) or (2), determines the probability that the radiation flux will pass through the cell without striking any foliage element. Thus, the proportion of flux contained in the radiation flux vector that passes through the cell can be expressed as $P_0(\phi,\theta)$ while the proportion of the flux that is attenuated—either absorbed or scattered—is given by $[1-P_0(\phi,\theta)]$. If the foliage absorption coefficient is a_f, then the proportion of the flux that is absorbed is $[1-P_0(\phi,\theta)]a_f$, while $[1-P_0(\phi,\theta)](1-a_f)$ is the proportion scattered. With the additional assumption that the spatial dispersions of the different types of foliage are independent of one another (Norman and Jarvis, 1976), the computation of successive attenuation of the radiant flux could be extended to any number of foliage components (e.g., thorns, flowers, fruit). In the current model, only leaves and stems are included so that, if F is the magnitude of the radiation flux vector as it enters the cell, then

$$A_l = F[1-P_0(\phi,\theta)]a_l \tag{6}$$

$$S_l = F[1-P_0(\phi,\theta)](1-a_l) \tag{7}$$

$$F' = FP_0(\phi,\theta) \tag{8}$$

are the fluxes absorbed (A_l), scattered (S_l) and unattenuated (F') by leaves while

$$A_s = F'[1-P_0(\phi,\theta)]a_s \quad (9)$$

$$S_s = F'[1-P_0(\phi,\theta)](1-a_s) \quad (10)$$

$$F'' = F'P_0(\phi,\theta) \quad (11)$$

are those fluxes absorbed (A_s), scattered (S_s) and unattenuated (F'') by stems. Summation of the above terms yields the initial flux, F, showing that the model conserves energy.

MODEL SENSITIVITY TO IRRADIANCE DISTRIBUTION

Vegetation architecture was specified for modules representing three types of natural vegetation: tropical rainforest, Sonoran desert and mid-latitude deciduous forest. Simulations then were performed for each of these modules to provide estimates of albedo as a function of the irradiance distribution. Model sensitivity to the irradiance distribution (i.e., solar zenith angle and percent diffuse) was determined for each of the vegetation types for each month of the year.

Vegetation Architecture

Required input data for the model consists of the following, defined for each cell containing vegetation: leaf and stem area densities; leaf and stem shortwave absorption coefficients; leaf and stem dispersion coefficients; leaf and stem backscatter parameters; and leaf and stem inclination angle distributions. In addition, the absorption coefficient for the substrate must be defined. None of these data were determined directly, but were instead estimated from observations reported in the literature. Complete input data are not presented here, but the leaf and stem area index profiles for each vegetation type are summarized graphically in Figure 3, and the seasonal variation of total leaf area index is given in Table 1. Some characteristics are common to all three vegetation types. First, foliage was assumed to be dispersed randomly throughout each cell containing foliage regardless of vegetation type. Although the model allows for regular and clumped foliage distributions as well as random, no quantitative data were available to estimate the required parameters for non-random dispersions. Second, substrate absorption coefficients were difficult to obtain, but did not vary greatly. A value of 0.75—representative of many soils (Sellers, 1965; Oke, 1987; Rosenberg et al., 1983) and characteristic of plant litter—was used for all three vegetation types.

Tropical Rainforest. Whitmore (1984) gives a plan view of a tropical lowland rainforest in Malaya that shows three stages of canopy development: gap, building and mature. Because an extensive area at the northern end of his study plot had been cleared, only the southern 100m was used to develop the module. This resulted in a 100x100m module that includes all three canopy phases. Since the individual trees that make up the tropical rainforest are large, a cell size measuring 10x10m in the horizontal was used to capture the horizontal variation in the

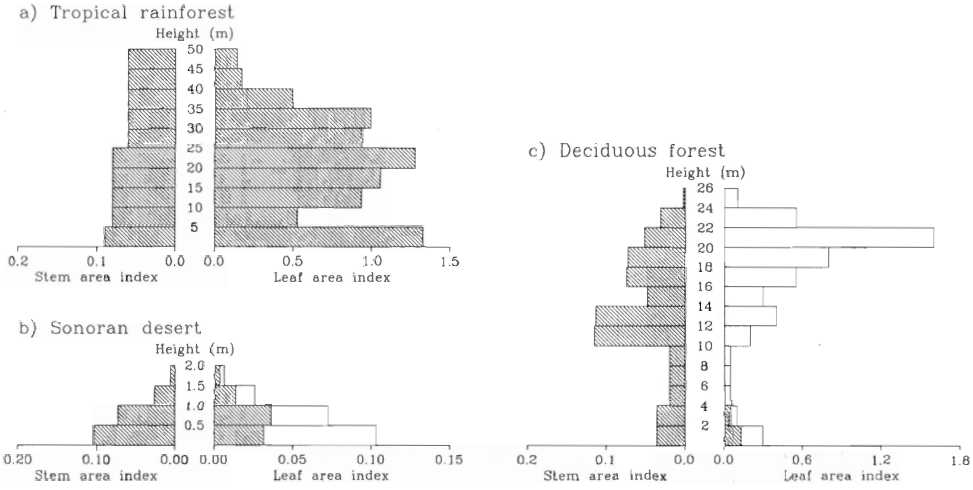

Fig. 3. Leaf area index profiles at minimum (shaded) and maximum (shaded + unshaded) total leaf area index and stem area index profiles for each vegetation module.

Table 1. Monthly Total Leaf Area Index and Total Stem Area Index (SAI) for Each Vegetation Module

	Leaf Area Index												SAI
Module	Jan	Feb	Mar	Apr	May	Jun	Jul	Aug	Sep	Oct	Nov	Dec	
Rainforest	7.89	7.89	7.89	7.89	7.89	7.89	7.89	7.89	7.89	7.89	7.89	7.89	0.71
Desert	0.08	0.12	0.15	0.17	0.19	0.21	0.19	0.17	0.19	0.10	0.09	0.10	0.21
Forest	0.18	0.18	0.31	2.24	4.59	5.05	5.05	5.05	4.57	1.65	0.67	0.18	0.63

canopy. For each cell, the dominant canopy phase—gap, building or mature—was determined.

Vertical distribution of foliage was derived from Kira (1978), who gives a profile of leaf area density in 5m layers based on clear felling of a forest strip. The canopy extends to 50m above the ground, with a dense layer between 20m and 35m. The upper limit was used as the height of the mature phase, while the lowest 5m (20–25m) of dense foliage marks the top of the building phase. The gap phase was assumed to occupy only the lowest 5m layer. Total leaf area derived from Kira's profile was distributed equally among all cells containing foliage in a layer. Leaf orientation in tropical rainforests is generally horizontal except in the uppermost portions of the canopy where the leaves tend to be vertical to avoid overheating (Brunig, 1983; Medina, 1983). This feature was approximated by giving cells in the top two layers of the mature phase as well as the top layer of the building phase a vertical leaf orientation distribution. All remaining cells were assumed to have horizontal leaves.

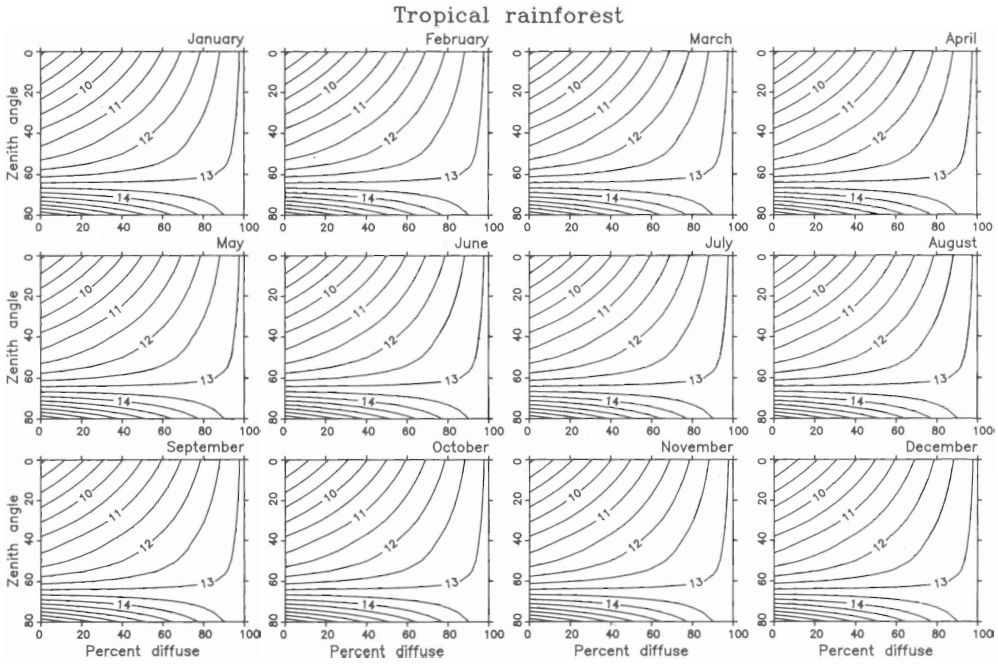

Fig. 4. Model output for tropical rainforest. Albedo is shown as a function of solar zenith angle and the diffuse fraction of total irradiance for each month of the year.

Determining the stem area density was more difficult as most vertical profiles of the woody portion of vegetation canopies are given in terms of biomass rather than surface area. Using an average trunk diameter of 0.5m (Unesco, 1978), the surface area of a cylinder, excluding the ends, was used to estimate stem area in each cell. Total surface area in the cell was divided by the cell volume to yield stem density, which was assumed constant throughout the canopy. Stems were assumed to be upright and so a vertical stem orientation distribution was used.

Little information on the optical properties of tropical rainforest leaves and stems was found in the literature. Chiariello (1984), in simulations of tropical leaf energy balances, gives a shortwave absorption coefficient for a "standard leaf" of 0.45; this value was adopted for the present study. Leaves of the tropical rainforest are generally thin so that the ratio of forward scatter to backscatter is close to unity. Absorption coefficients for stems were even more difficult to obtain than those for leaves. Only a single stem absorption coefficient was found in the literature (Roberts and Miller, 1977) and this value (a_s=0.85) was adopted for stems of all three vegetation types.

While tropical rainforest trees drop their leaves and grow new foliage throughout the year, the canopy as a whole experiences little seasonal variation in leaf area index (Walter, 1971). Therefore, no seasonal changes were introduced into this module.

Sonoran desert. Desert plants are often assumed to be regularly distributed in space as a result of competition for moisture. However, in a review of several earlier studies, Barbour (1973) found that a random distribution of desert plants is more common. For this reason, individual shrubs were placed randomly in a 10x10m area until total ground cover reached 20 percent (Chew and Chew, 1965). Cell dimensions were set to 0.5x0.5x0.5m to account for the vegetation architecture. Shrub heights were taken from the height classes of Barbour et al. (1977) and then were adjusted to be consistent with the 0.5m cell height. Individual shrubs were assumed to have a diameter equal to their height and were given a somewhat "rounded" shape.

Two shrub species were assumed to occur in this community—a large, dominant, evergreen shrub and a smaller, short-lived, drought-deciduous shrub. Both species were assumed to have the same peak leaf area density, but their phenologies differ. Total leaf area index for this desert community is low; but, with only a small volume occupied by foliage, leaf area densities in foliated cells are commensurate with those of "denser" vegetation types (e.g., deciduous forest). Stem area densities were assumed equal to peak leaf area densities and both leaves and stems were assigned a spherical orientation distribution.

Leaf optical properties were derived from the observations of Ehleringer (1981) and his relationship for converting visible absorptance to total shortwave absorptance. Ehleringer (1981) also notes that leaf transmittance is low for most desert plants so the ratio of forward to backscatter is small.

Seasonal changes in leaf area density for the evergreen shrub are based on the description of Chew and Chew (1965). During June through August, these shrubs bear two years' growth of leaves, the older of which are shed during September and October. New leaves develop during the spring (March through May). Therefore, leaf area densities during winter (one year's growth) were assumed to be half of the peak summer density (two years' growth) with transition periods in the spring and fall. Seasonal changes in leaf area density of the deciduous shrub are more pronounced in response to moisture availability. An observed phenology for 1971 (Ackerman and Bamberg, 1974) was used to estimate the phenology for the drought-deciduous shrubs.

Deciduous forest. A module area of 18x18m containing nine large individual trees was used to give a stand density (275 stems ha^{-1}) representative of a mature deciduous forest (DeAngelis, Gardner and Shugart, 1981). The module was divided into 2x2x2m cells to capture the variability within the stand. Individual trees, with crowns approximated by ellipsoids (6m in diameter and 10m long), were placed randomly within the module. Crowns were not allowed to intersect. Crowns of adjacent trees, however, were allowed to touch and a higher layer of one crown could overtop a lower layer of another, but a single cell could not be occupied by the crowns of two trees. Tree heights were based on a height distribution function derived from stand heights in the Woodlands Data Set (DeAngelis, Gardner and Shugart, 1981). Small trees, saplings and deciduous and evergreen shrubs were included in the understory in sufficient numbers to yield appropriate coverage (Falinski, 1986).

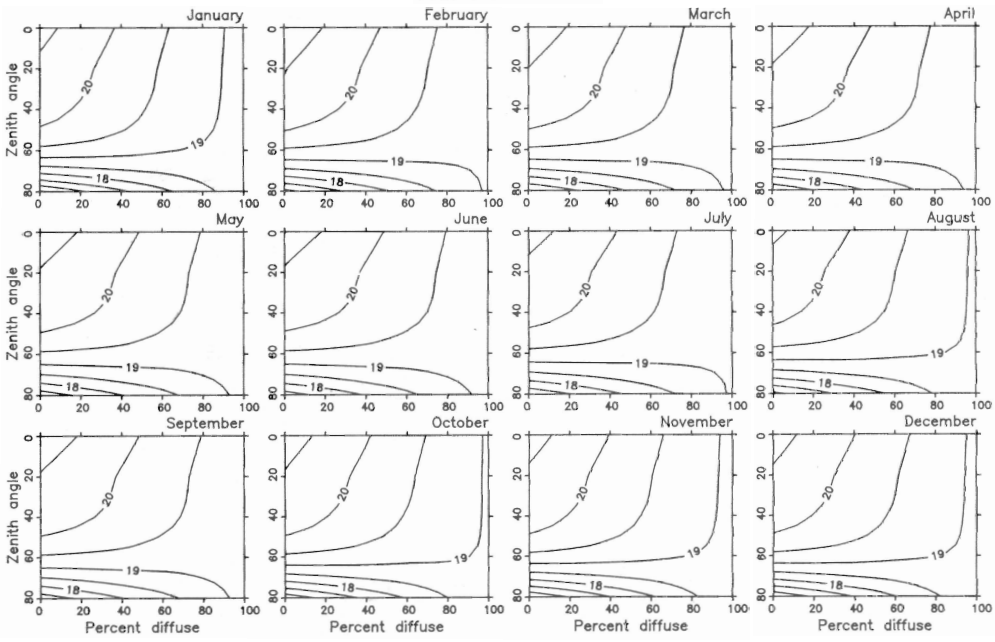

Fig. 5. Model output for Sonoran desert. Albedo is shown as a function of solar zenith angle and the diffuse fraction of total irradiance for each month of the year.

The vertical distributions of leaf and stem area were taken from the profiles of mean layer area densities given by Hutchinson et al. (1986). These values were converted to total leaf areas in each 2m layer, then divided by the total volume of foliated cells in that layer to give actual leaf area density of those cells. Small trees occupying a layer containing mature trees were assumed to have a leaf area density half that of the mature trees in that layer. Mature trees were assumed to have spherical leaf orientation distributions while the smaller trees, saplings and shrubs occupying the darker, lower levels of the module were assumed to have horizontal leaves (Hutchinson et al., 1986). Stem orientation was assumed to be vertical for all trees (Hutchinson et al., 1986) while, for shrubs, it was assumed to be spherical.

Deciduous leaf absorptance, including its seasonal variation, was estimated using data for numerous deciduous species throughout the growing season (Gates, 1980). Since most broad deciduous leaves are thin, the ratio of forward to backscatter should be close to unity (Gates, 1980).

Phenological studies of deciduous forests are numerous. Generally, leaf emergence occurs in the early spring and leaf area densities reach a maximum by late spring. Leaf fall begins in late summer, reaches a maximum in early to mid-autumn and usually is complete by late autumn (Taylor, 1974). In some cases, the dead leaves remain on the tree through the winter, not falling until the new crop begins to emerge in the spring. Deciduous shrubs often begin to develop new leaves earlier in the spring than do overstory trees (Taylor, 1974), perhaps to take

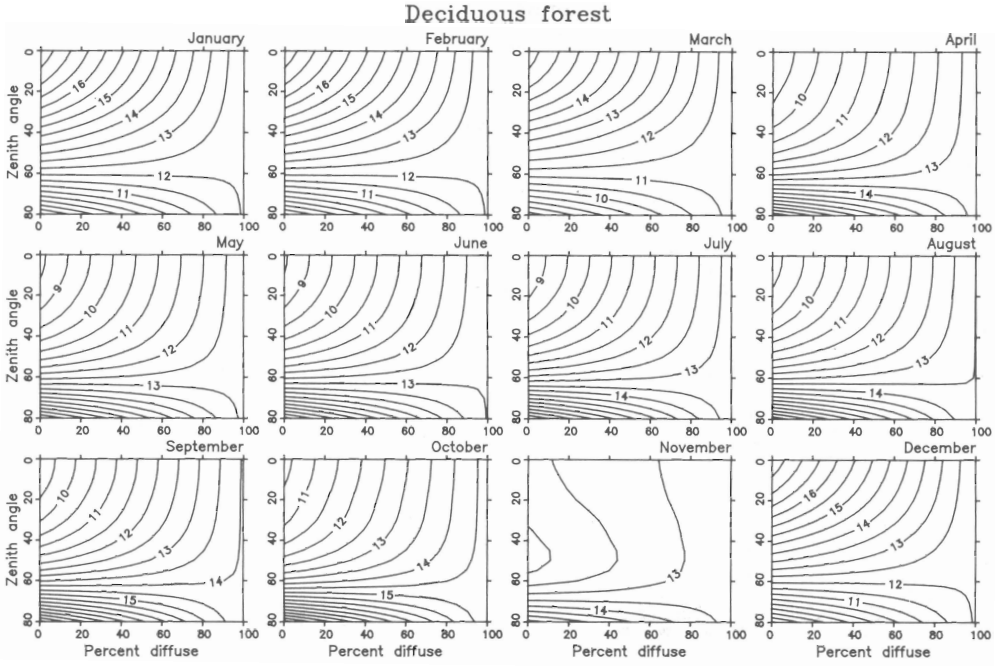

Fig. 6. Model output for deciduous forest. Albedo is shown as a function of solar zenith angle and the diffuse fraction of total irradiance for each month of the year.

advantage of available radiation prior to canopy closure. A slight variation in leaf area density was included for evergreen shrubs to account for annual growth and loss of leaves.

Irradiance Distribution

The prescribed irradiance distribution was composed of two components: an isotropically-distributed diffuse component and a beam component. Beam was varied from 0 to 100 percent of the total in increments of 20 percent, while the solar zenith angle was changed from 0° (directly overhead) to 80° (near the horizon) in 200 steps. Zenith angle increments of 20° are equal to the interval ($\Delta\,\theta$) used to define the paths along which radiant flux propagates in the model. The azimuth increment ($\Delta\,\phi$) was 30° yielding a total of 98 radiation source vectors. Because the vegetation modules were not defined with strict reference to the cardinal directions, the dependence of albedo on the solar azimuth was not investigated. Rather, the solar azimuth was held constant at 120°—chosen so that beam radiation would not be parallel to the horizontal axes of the vegetation cells.

The sensitivity experiment yielded albedo estimates that are, in many respects, consistent with previous observations of albedo dependence on irradiance distribution. As Henderson-Sellers and Wilson (1983, pp. 1752–1753) noted:

> for vegetated surfaces, especially where the canopy structure is vertical, minimum albedo occurs when incoming radiation is direct radiation coming from overhead (low zenith) and maximum trapping of radiation by multiple reflection occurs. As the zenith angle increases, the multiple reflection within the canopy decreases, and more radiation is reflected off the top of the canopy.

This effect can be seen, for example, in the model results for tropical rainforest (Fig. 4). For regions of sparse vegetation, such as the Sonoran Desert (Fig. 5), an opposite trend is apparent. This is because the underlying substrate generally has a higher albedo than does the vegetation and radiation from near the zenith reaches this substrate more easily than does radiation from near the horizon. Low vegetation density and limited vertical development also reduce the importance of light trapping. When vegetation is extremely sparse, no trend is apparent and the surface behaves very nearly as a Lambertian reflector. In vegetation with a significant deciduous component, the trend may reverse seasonally as the foliage density changes (Fig. 6).

For an isotropic distribution of irradiance, radiation reaches the top of the canopy with an average zenith angle of 60° and thus, for homogeneous canopies, the albedo for isotropic irradiance should be equal to that of beam irradiance at a zenith angle of 60°. While none of the vegetation modules is completely homogeneous, the more nearly homogeneous modules clearly approach this relationship (e.g., Figs. 4 and 6).

While these results show that the model is able to reproduce observed trends—with respect to solar zenith angle and diffuse irradiance variations—it remains to be shown that the magnitudes are reasonable.

COMPARISON TO PREVIOUSLY TABULATED ALBEDOS

In order to show that the model estimates albedos of the proper magnitude, it is necessary to compare the modeled albedos with those obtained through independent observations. For the model to be validated completely, however, these independently obtained albedo data must be accompanied by information on the incident radiation distribution and descriptions of the vegetation architecture that are sufficient to drive the model. Kukla (1981), in his review of the effects of land-surface albedo on climate variations, recognized that "existing data are inadequate and incomplete" at least in part because of the lack of details about the atmospheric and surface conditions at the time of observation. No entirely adequate validation data set exists and only less-than-optimal comparisons can be made between modeled and observed albedos.

One of the more complete vegetation albedo data sets compiled to date is that of Matthews (1983, 1984). She derived seasonal albedos for each of 32 land-cover categories under snow-free conditions (except for permanently snow- or ice-covered surfaces) from the literature. Direct comparison of these data with the results of the model simulations, however, is difficult for several reasons. First, Matthews' data are given seasonally while the present simulations are monthly.

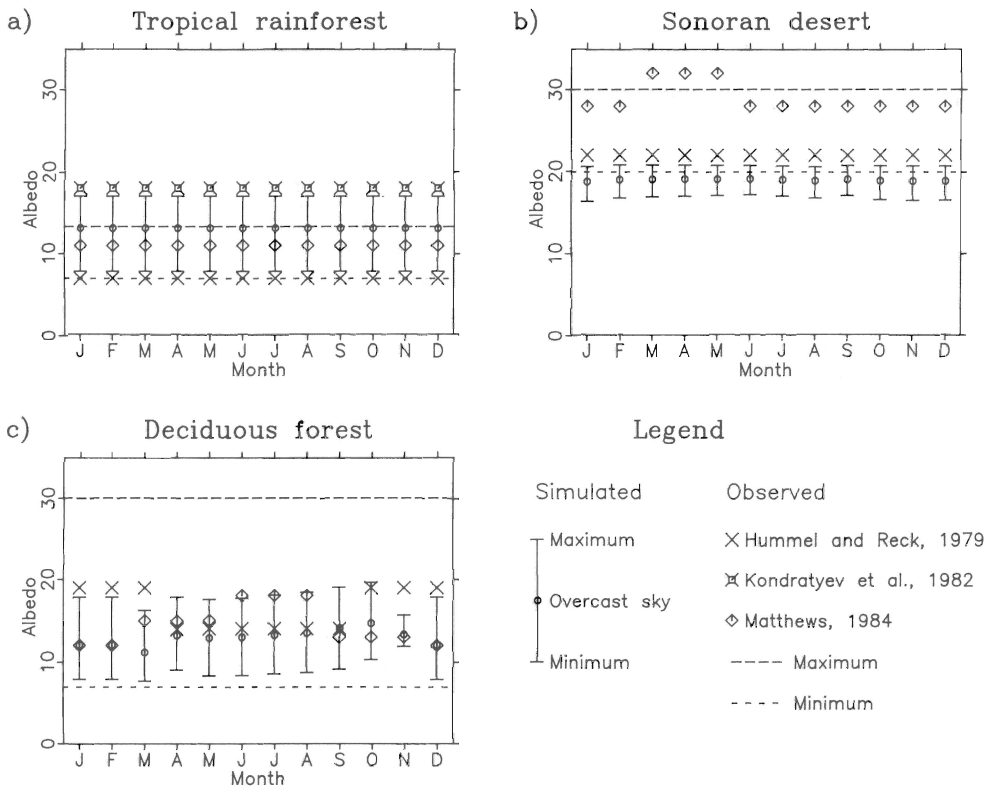

Fig. 7. Comparison between model output and observed albedos.

Second, Matthews' albedos do not account explicitly for variations caused by solar zenith angle and diffuse irradiance distribution. Finally, Matthews does not provide sufficient description of the vegetation architecture and meteorological conditions at the time of observation.

Despite these problems, Matthews' albedo data are probably the best currently available and so they will be used to assess the validity of the simulated albedos. In addition to Matthews' data, the more limited seasonal albedo tabulations of Hummel and Reck (1979) and Kondratyev et al. (1982) are used, where applicable. These compilations have many of the same problems as Matthews' archive; that is, seasonal albedos only, no variation with changing irradiance distribution and no information on vegetation architecture or concurrent meteorological conditions. Additional albedo observations for the different vegetation types were obtained from the literature. Once again, the vegetation canopy and meteorological conditions at the time of observation are not reported. Nevertheless, these albedos should approximate the range of values encountered for a given vegetation assemblage.

Comparison of simulated monthly albedos with the various observed albedos can best be made graphically. Because the model estimates the variation of albedo with changing solar zenith angle and percent diffuse irradiance, the maximum and

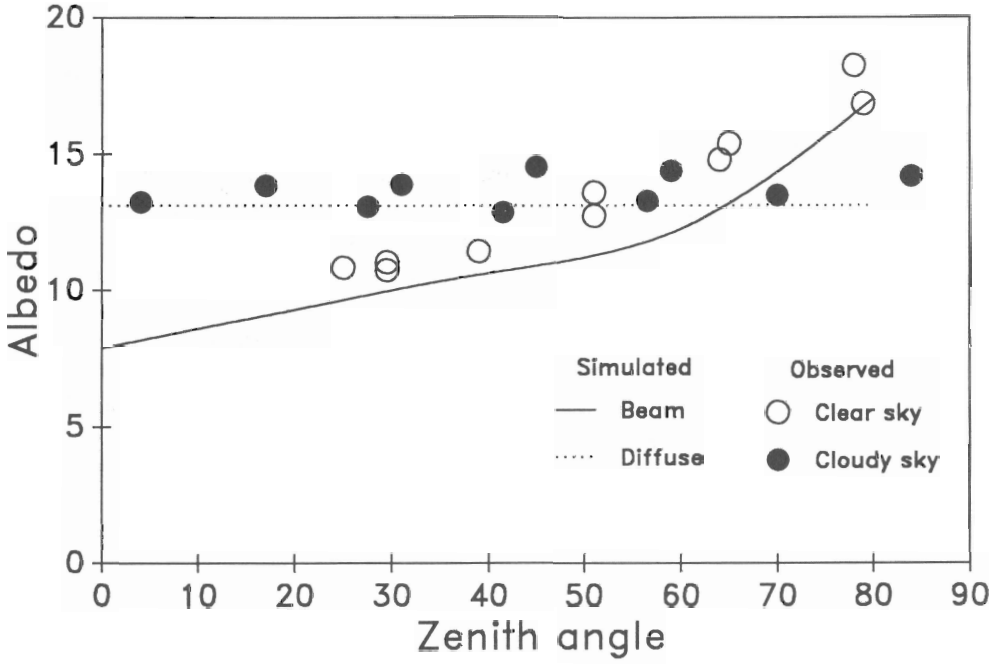

Fig. 8. Zenith angle dependence of the albedo of a tropical rainforest. Simulation results are shown for a range of diffuse fractions and observations are given for clear (○) and cloudy (●) conditions (Pinker, 1982).

minimum albedos predicted by the model are shown (Fig. 7). These extreme values always occur under conditions of little or no diffuse radiation and, therefore, the simulated albedos under overcast skies (i.e., totally diffuse irradiance) are also shown. Seasonal albedos reported by Matthews (1983, 1984) are plotted for each vegetation type and are supplemented by the data of Hummel and Reck (1979) and Kondratyev et al. (1982) as well as by the range of albedos found in the literature, whenever these data are available.

Tropical Rainforest

Most estimates of the albedo of tropical rainforest vegetation, including those of Hummel and Reck (1979), Kondratyev et al. (1982) and Matthews (1984), assume that there is no seasonal variation. Albedos predicted by the model, however, vary depending on the angular distribution of irradiance (Fig. 7a) even though the canopy architecture is held constant over the year. Therefore, both seasonal and diurnal (Pinker et al., 1980; Pinker, 1982) variations caused by changing solar zenith angle can be predicted by the model (Fig. 8). Finally, the range of albedos simulated corresponds well to the range of observed albedos.

Sonoran Desert

For sparse vegetation, the absorption coefficient specified for the substrate is critical in determining the simulated albedo. Soils of the Sonoran desert consist primarily of loams with different proportions of rocky material (MacMahon and Wagner, 1985). Sellers (1965) specifies the albedo of dry clay or gray soils as 0.20–0.35; the presence of loose rocks on the surface would further decrease the albedo. Therefore, a value of 0.25 was adopted for the substrate albedo in this desert shrubland. The results obtained for this canopy (Fig. 7b) are near or below the minimum albedos found in the literature. Increasing the substrate albedo used in the simulations would increase the predicted albedos; while this would produce better agreement with observed albedos, it cannot be justified on physical grounds. Matthews' albedos appear to be too high; in fact, her spring albedos exceed the values she assigns to desert (Matthews, 1984) as well as the highest albedos cited in the literature for shrub deserts. Since she does not document the source(s) of her values, it is impossible to judge their validity for the Sonoran desert.

Deciduous Forest

Model-predicted albedos for deciduous forest agree well with those found in the literature (Fig. 7c). When zenith angle effects (Fig. 6) are considered, the model predicts lower albedos in the summer (i.e., higher zenith angles) when the forest is fully leafed. This agrees with the seasonal trend given by Hummel and Reck (1979) but is opposite to that of Matthews (1984).

Because a fully-leafed canopy should trap more radiation than an open canopy, summer albedos should be lower than winter albedos for a deciduous forest. Results reported by Baldocchi et al. (1984) for an oak-hickory forest in eastern Tennessee support this hypothesis. Rauner (1976), however, reported that the albedo of some deciduous forests increases from spring to summer, with the maximum albedo occurring during the fully-leafed period, thus supporting the seasonal variation given by Matthews (1984). These apparently contradictory results, as well as the large range of albedos cited in the literature, could be due largely to the degree of canopy closure. The simulated forest as well as the oak-hickory forest investigated by Baldocchi et al. have almost completely closed canopies; neither Matthews nor Rauner specifies the degree of canopy closure.

SUMMARY AND CONCLUSIONS

Surface albedo determines the proportion of incident solar radiation that is absorbed by the surface. Because the troposphere is heated primarily by energy fluxes arising from the surface rather than by absorption of solar radiation, the surface albedo plays an important role in climate processes.

A primary determinant of the land-surface albedo is the Earth's vegetation cover, which presents numerous absorbing and scattering surfaces to the incident

radiation. The interaction of radiation with vegetation canopies is dependent upon many factors including the angular distribution and spectral composition of the radiation, the optical properties of the foliage and substrate, the spatial and angular distribution of the foliage and the architecture of the canopy. Because of these complex dependencies, observations of vegetation albedo are unlikely to represent the full range of possible interactions. However, current climate models rely upon these vegetation albedo observations to prescribe the land-surface albedo in climate simulations.

A model of radiation transfer in vegetation canopies was used in an attempt to overcome the deficiencies of albedo observations. This model incorporates explicitly the optical properties and physical characteristics of a vegetation stand to predict the albedo of the stand under a specified irradiance distribution. In contrast to other large-scale characterizations of albedo, the present model predicts vegetation albedos that are, in general, different under clear-sky and overcast conditions. Moreover, the model is able to simulate the well-documented diurnal variation in albedo caused by changing solar zenith angle.

Simulations confirm that the model is able to predict quite well the variation of albedo under different distributions of incident radiation. These simulated albedos, however, are often different in magnitude from those observed. This can be attributed to several factors including: (1) differences between the actual vegetation architecture at the time of observation and the canopy architecture used by the model, (2) the lack of information regarding the irradiance distribution when the observations were made, (3) incorrect specification of foliage dispersion, orientation and optical properties, and (4) incorrect parameterization, especially for sparse vegetation, of the optical properties of the substrate. The simulation results, nonetheless, are encouraging since—with improved data on the architecture of vegetation canopies and better observations of vegetation albedo—close agreement between observed and model-predicted albedos seems possible.

BIBLIOGRAPHY

Ackerman, T.L. and Bamberg, S.A. (1974) Phenological studies in the Mojave Desert at Rock Valley (Nevada Test Site). In H. Leith, ed., *Phenological and Seasonality Modeling*, Ecological Studies No. 8. New York: Springer-Verlag, 215–226.

Baldocchi, D.D., Matt, D.R., Hutchinson, B.A., and McMillen, R.T. (1984) Solar radiation within an oak-hickory forest: an evaluation of the extinction coefficients for several radiation components during fully-leafed and leafless periods. *Agric. Forest Meteorol.*, Vol. 32, 307–322.

Barbour, M.G. (1973) Desert dogma reexamined: root/shoot productivity and plant spacing. *Amer. Midl. Nat.*, Vol. 89, 41–57.

_____, MacMahon, J.A., Bamberg, S.A., and Ludwig, J.A. (1977) The structure and distribution of *Larrea* communities. In T.J. Mabry, J.H. Hunziker, and D.R. DiFeo, eds., *Creosote Bush: Biology and Chemistry of Larrea in New World Deserts*, US/IBP Synthesis Series No. 6. Stroudsburg, PA: Dowden, Hutchinson and Ross, 227–251.

Brunig, E.F. (1983) Vegetation structure and growth. In F.B. Golley, ed., *Tropical Rain Forest Ecosystems*, Ecosystems of the World No. 14A. Amsterdam: Elsevier Scientific, 49–75.

Carson, D.J. (1982) Current parameterizations of land-surface processes in atmospheric general circulation models. In P.S. Eagleson, ed., *Land Surface Processes in Atmospheric General Circulation Models*. Cambridge: Cambridge University Press, 67–108.

Charney, J.G., Quirk, W.J., Chow, S-M. and Kornfield, J. (1977) A comparative study of the effects of albedo change on drought in semi-arid regions. *J. Atmos. Sci.*, Vol. 34, 1366–1385.

Chew, R.M. and Chew, A.E. (1965) The primary productivity of a desert-shrub (*Larrea tridentata*) community. *Ecol. Monogr.*, Vol. 35, 355–375.

Chiariello, N. (1984) Leaf energy balance in the wet lowland tropics. In E. Medina, H.A. Mooney, and C. Vazquez-Yanes, eds., *Physiological Ecology of Plants in the Wet Tropics*, Tasks for Vegetation Science No. 12. The Hague: Dr W Junk Publ., 85–98.

Coakley, J.A. and Chylek, P. (1975) The two-stream approximation in radiative transfer: including the angle of incident radiation. *J. Atmos. Sci.*, Vol. 32, 409–418.

Cooper, K., Smith, J.A. and Pitts, D. (1982) Reflectance of a vegetation canopy using the Adding method. *Appl. Opt.*, Vol. 21, 4112–4118.

DeAngelis, D.L, Gardner, R.H., and Shugart, H.H. (1981) Productivity of forest ecosystems studied during IBP: the woodlands data set. In D.E. Reichle, ed., *Dynamic Properties of Forest Ecosystems*, International Biological Programme, No. 23. Cambridge: Cambridge Univ. Press, 567–672.

Dickinson, R.E. (1983) Land surface processes and climate—surface albedo and energy balance. *Advances in Geophysics*, Vol. 25, 305–353.

_____ and Hanson, B. (1984) Vegetation-albedo feedbacks. In J.E. Hansen and T. Takahasi, eds., *Climate Processes and Climate Sensitivity*, Geophysical Monograph 29, Maurice Ewing Volume 5. Washington, D.C.: American Geophysical Union, 180–186.

Ehleringer, J. (1981) Leaf absorptances of Mohave and Sonoran desert plants. *Oecologia (Berl.)*, Vol. 49, 366–370.

Falinski, J.B. (1986) *Vegetation Dynamics in Temperate Lowland Primeval Forests*. Dordrecht: Dr W Junk Publ.

Federer, C.A. (1971) Solar radiation absorption by leafless hardwood forests. *Agric. Meteorol.*, Vol. 9, 3–20.

Gates, D.M. (1980) *Biophysical Ecology*. New York: Springer-Verlag.

Henderson-Sellers, A. and Wilson, M.F. (1983) Surface albedo data for climatic modeling. *Rev. Geophys. Space Phys.*, Vol. 21, 1743–1778.

Hummel, J.R. and Reck, R.A. (1979) A global surface albedo model. *J. Appl. Meteorol.*, Vol. 18, 239–253.

Hutchinson, B.A., Matt, D.R., McMillan, R.T., Gross, L.J., Tjachman, S.J. and Norman, J.M. (1986) The architecture of a deciduous forest canopy in eastern Tennessee, U.S.A. *J. Ecol.*, Vol. 74, 635–646.

Kimes, D.S. (1984) Modeling the directional reflectance from complete homogeneous vegetation canopies with various leaf-orientation distributions. *J. Opt. Soc. Am., A,* Vol. 1, 725–737.

_____ and Kirchner, J.A. (1982) Radiative transfer model for heterogeneous 3-D scenes. *Appl. Opt.,* Vol. 21, 4119–4129.

Kira, T. (1978) Community architecture and organic matter dynamics in tropical lowland rain forests of Southeast Asia with special reference to Pasoh Forest, West Malaysia. In P.Z. Tomlinson and M.H. Zimmerman, eds., *Tropical Trees as Living Systems.* Cambridge: Cambridge Univ. Press, 561–590.

Kondratyev, K.Ya., Korzov, V.I., Mukhenberg, V.V. and Dyachenko, L.N. (1982) The shortwave albedo and the surface emissivity. In P.S. Eagleson, ed., *Land Surface Processes in Atmospheric General Circulation Models.* Cambridge: Cambridge University Press, 463–514.

Kuchler A.W. (1978) Natural vegetation. In E.B. Espenshade and J.L. Morrison, eds., *Goode's World Atlas,* fifteenth edition. Chicago: Rand McNally, 16–17.

Kukla, G. (1981) Surface albedo. In A. Berger, ed., *Climate Variations and Variability.* Dordrecht: D. Reidel, 85–109.

MacMahon, J.A. and Wagner, F.H. (1985) The Mojave, Sonoran and Chihuahuan deserts of North America. In M. Evanari, I. Noy-Meir, and D.W. Goodall, eds., *Hot Deserts and Arid Shrublands,* Ecosystems of the World No. 12A. Amsterdam: Elsevier Scientific, 105–202.

Matthews, E. (1983) Global vegetation and land use: new high-resolution data bases for climate studies. *J. Climate Appl. Meteorol.,* Vol. 22, 474–487.

_____ (1984) Vegetation, land-use and seasonal albedo data sets: documentation of archived data tape. *NASA Tech. Memo. 86107.*

Meador, W.E. and Weaver, W.R. (1980) Two-stream approximations to radiative transfer in planetary atmospheres: a unified description of existing methods and a new improvement. *J. Atmos. Sci.,* Vol. 37, 630–643.

Medina, E. (1983) Adaptations of tropical trees to moisture stress. In F.B. Golley, ed., *Tropical Rain Forest Ecosystems,* Ecosystems of the World No. 14A. Amsterdam: Elsevier Scientific, 225–237.

Nilson, T. (1971) A theoretical analysis of the frequency of gaps in plant stands. *Agric. Meteorol.,* Vol. 8, 25–38.

Norman, J. and Jarvis, P.G. (1976) Photosynthesis in Sitka spruce (*Picea sitchensis* (Bong.) Carr.) V. Radiation penetration theory and a test case. *J. Appl. Ecol.,* Vol. 13, 839–878.

Oke, T.R. (1987) *Boundary Layer Climates,* second editon. London: Methuen.

Pinker, R.T. (1982) The diurnal asymmetry in the albedo of tropical forest vegetation. *Forest Sci.,* Vol. 28, 297–304.

Pinker, R.T., Thompson, O.E. and Eck, T.F. (1980) The albedo of a tropical evergreen forest. *Quart. J. Roy. Meteorol. Soc.,* Vol. 106, 551–558.

Potter, G.L., Ellsaesser, H.W., MacCracken, M.C., and Ellis, J.S. (1981) Albedo change by man: test of climatic effects. *Nature,* Vol. 291, 47–50.

Preuss, H. and Geleyn, J.F. (1980) Surface albedoes derived from satellite data and their impact on forecast models. *Arch. Meteorol. Geophys. Biokl., Ser. A,* Vol. 29, 345–356.

Rauner, Ju.L. (1976) Deciduous forest. In J.L. Monteith, ed., *Vegetation and the Atmosphere, Volume 2: Case Studies.* London: Academic Press, 241–264.

Roberts, S.W. and Miller, P.C. (1977) Interception of solar radiation as affected by canopy organization in two mediterranean shrubs. *Oecol. Plant.*, Vol. 12, 273–290.

Rosenberg, N.J., Blad, B.L., and Verma, S.B. (1983) *Microclimate: The Biological Environment*, second edition. New York: Wiley.

Ross, J. (1975) *The Radiation Regime and Architecture of Plant Stands.* The Hague: Dr W. Junk Publ.

Sellers, P.J. (1985) Canopy reflectance, photosynthesis and transpiration. *Int. J. Rem. Sens.*, Vol. 6, 1335–1372.

Sellers, W.D. (1965) *Physical Climatology.* Chicago: Univ. of Chicago Press.

Taylor, F.G. (1984) Phenodynamics of production in a mesic deciduous forest. In H. Leith, ed., *Phenology and Seasonality Modeling*, Ecological Studies No. 8. New York: Springer-Verlag, 237–254.

UNESCO (1978) *Tropical Forest Ecosystems*, Natural Resources Research Series No. 14. Paris: UNESCO.

Walter, H. (1971) *Ecology of Tropical and Subtropical Vegetation* (D. Mueller-Dombois, transl.; J.H. Burnett, ed.). New York: Van Nostrand Reinhold.

Warren Wilson, J. (1961) Influence of spatial arrangement of foliage area on light interception and pasture growth. *Proc. 15th Int. Grassl. Conf.*, 275–279.

Whitmore, T.C. (1984) *Tropical Rain Forests of the Far East*, second edition. Oxford: Clarendon Press.